

Membrane-directed molecular assembly of the neuronal SNARE complex

Won Jin Cho ^a, Jin-Sook Lee ^a, Lei Zhang ^{c, b}, Gang Ren ^{b, †}, Leah Shin ^a, Charles W. Manke ^c,
Jeffrey Potoff ^c, Nato Kotaria ^d, Mzia G. Zhvania ^{d, e}, Bhanu P. Jena ^{a, c, *}

^a Department of Physiology, Wayne State University School of Medicine, Detroit, MI, USA

^b Department of Biochemistry and Biophysics, University of California-San Francisco, San Francisco, CA, USA

^c Department of Chemical Engineering and Materials Science, Wayne State University, College of Engineering, Detroit, MI, USA

^d I. Beritashvili Institute of Physiology of Georgia, Tbilisi, Georgia

^e I. Chavchavadze State University, Tbilisi, Georgia

[†] Lawrence Berkeley National Laboratory, Berkeley, CA, USA

Received: May 12, 2010; Accepted: July 5, 2010

Abstract

Since the discovery and implication of N-ethylmaleimide-sensitive factor (NSF)-attachment protein receptor (SNARE) proteins in membrane fusion almost two decades ago, there have been significant efforts to understand their involvement at the molecular level. In the current study, we report for the first time the molecular interaction between full-length recombinant t-SNAREs and v-SNARE present in opposing liposomes, leading to the assembly of a t-/v-SNARE ring complex. Using high-resolution electron microscopy, the electron density maps and 3D topography of the membrane-directed SNARE ring complex was determined at nanometre resolution. Similar to the t-/v-SNARE ring complex formed when 50 nm v-SNARE liposomes meet a t-SNARE-reconstituted planer membrane, SNARE rings are also formed when 50 nm diameter isolated synaptic vesicles (SVs) meet a t-SNARE-reconstituted planer lipid membrane. Furthermore, the mathematical prediction of the SNARE ring complex size with reasonable accuracy, and the possible mechanism of membrane-directed t-/v-SNARE ring complex assembly, was determined from the study. Therefore in the present study, using both liposome-reconstituted recombinant t-/v-SNARE proteins, and native v-SNARE present in isolated SV membrane, the membrane-directed molecular assembly of the neuronal SNARE complex was determined for the first time and its size mathematically predicted. These results provide a new molecular understanding of the universal machinery and mechanism of membrane fusion in cells, having fundamental implications in human health and disease.

Keywords: membrane-associated SNARE ring complex • electron 3D topography • atomic force microscopy

Introduction

The self-assembly of supramolecular structures is vital to numerous life processes, such as membrane fusion. Neurotransmission, and the secretion of hormones or digestive enzymes, involve fusion of opposing cellular membranes. At the nerve terminal, target membrane proteins synaptosomal-associated protein 25 (SNAP-25) and syntaxin 1A termed t-SNAREs, and synaptic vesicle (SV)-associated membrane protein VAMP2 or v-SNARE, are part of the

conserved proteins involved in fusion of opposing cellular membranes [1–3]. In the presence of Ca²⁺, when a v-SNARE-vesicle meets a t-SNARE reconstituted planar lipid membrane, SNAREs in opposing membranes interact and self-assemble in a ring, establishing continuity between the opposing compartments [4]. Size of the SNARE ring is directly proportional to the size of the v-SNARE-associated vesicle [5]. In contrast, SNAREs deprived of membrane fail to assemble in a ring [4]. The key to our understanding of SNARE-induced membrane fusion requires determination of the atomic arrangement and interaction between membrane-associated v- and t-SNAREs. Ideally, the atomic coordinates of membrane-associated SNARE complex using x-ray crystallography would help elucidate the chemistry of SNARE-induced membrane fusion in cells. Unfortunately, such structural details at the atomic level of membrane-associated t-/v-SNARE complex have not been

*Correspondence to : Bhanu P. JENA, Ph.D.,
Department of Physiology,
Wayne State University School of Medicine,
540 E. Canfield, 5245 Scott Hall, Detroit, MI 48201, USA.
Tel.: 313-577-1532
Fax: 313-993-4177
E-mail: bjena@med.wayne.edu

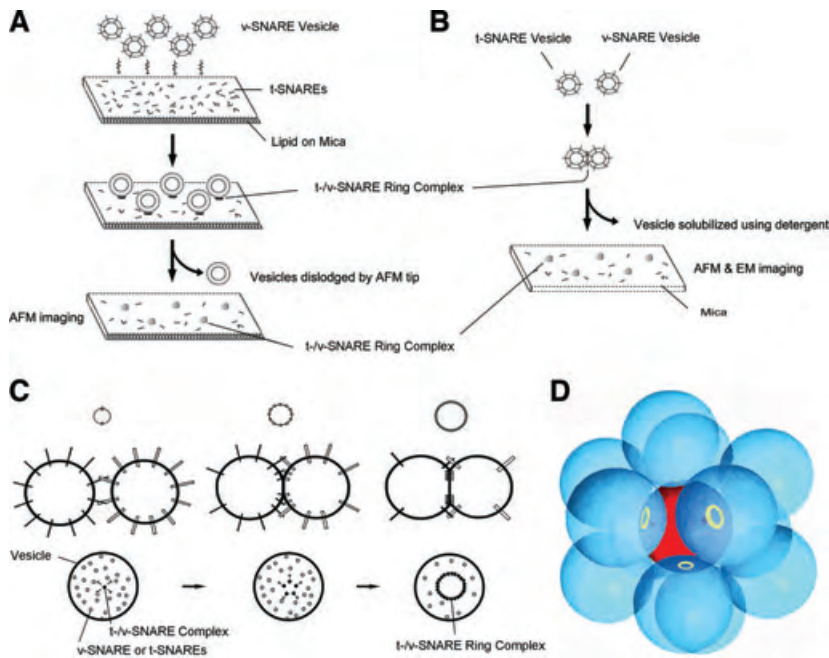


Fig. 1 Schematic flow diagram establishing membrane-associated SNARE complex assembly and its structural evaluation using AFM and EM. **(A)** Preteoliposomes of a specific size containing v-SNARE can be exposed to t-SNARE-reconstituted lipid membrane supported by a mica surface. The interaction results in the formation of a highly stable t-/v-SNARE ring complex which can be observed using AFM following removal of the vesicle. **(B)** Similarly, proteoliposomes of a certain size, one reconstituted with v-SNARE and the other with t-SNARE, can interact **(C, D)** to form membrane-directed t-/v-SNARE complex. However, in this situation, a single t-SNARE vesicle (red) is physically limited to establish contact with a maximum of 12 (blue) equal-size v-SNARE vesicles, and vice versa. This allows for approximately no more than 6% of the total surface area of one vesicle to interact with others, translating the membrane-directed t-/v-SNARE complex to be just around 6% of the total. In order to observe this membrane-directed SNARE complex, the liposomes are solubilized using detergent, and the stable t-/v-SNARE ring complex formed as a result of membrane-directed assembly, is then

imaged using AFM and EM. **(C)** Schematic diagram depicting the possible molecular mechanism of SNARE ring complex formation, when t-SNARE-vesicles and V-SNARE-vesicles meet. The process may occur due to a progressive recruitment of t-/v-SNARE pairs as the opposing vesicles are pulled toward each other, until a complete ring is established, preventing any further recruitment of t-/v-SNARE pairs to the complex. The top panel is a side view of two vesicles (one t-SNARE-reconstituted, and the other v-SNARE reconstituted) interacting to form a single t-/v-SNARE complex, leading progressively (from left to right) to the formation of the ring complex. The lower panel is a top view of the two interacting vesicles.

possible, primarily due to solubility problems of membrane-associated SNAREs and because v-SNARE and t-SNAREs need to reside in opposing membranes when they meet to be able to assemble in a physiologically relevant conformation. The remaining option has been the use of nuclear magnetic resonance spectroscopy (NMR), which too has been unsuccessful due to the size of the t-/v-SNARE complex being larger than current NMR capabilities. Regardless of these setbacks, atomic force microscopy (AFM) has provided, at nanometre resolution, an understanding of the structure [4, 5]. Because membrane association of SNAREs is critical to their assembly and function, the molecular conformations in the assembly and disassembly of full length SNAREs both in buffered suspension and in membrane, have been previously examined using circular dichroism (CD) spectroscopy [6]. Results from the CD study demonstrate that the α -helices both within v-SNARE and t-SNAREs, and their complexes, are significantly less pronounced when membrane-associated than in suspension. Furthermore, exposure of the t-/v-SNARE-NSF complex to ATP, results in dissociation of α -helices present within the SNARE complex, as also demonstrated using AFM [7].

Because majority of intracellular fusion events occur between vesicular compartments, it was imperative to determine the structure and arrangement of the t-/v-SNARE complex when t-SNARE-vesicles and v-SNARE-vesicles meet. In this case, because both opposing membrane would exhibit curvature, we expected the v- and t-SNAREs to interact at a point, attracting additional SNARE

pairs to form a t-/v-SNARE bundle. To test our hypothesis, two sets of 50 nm diameter liposomes were reconstituted with t-SNAREs and v-SNARE respectively (Fig. 1A–C), for use in our study. Surprisingly, exposure of 50 nm v-SNARE-liposome to 50 nm t-SNARE-liposome resulted in the establishment of a highly stable approximately 8 nm diameter t-/v-SNARE ring complex. Once formed, the t-/v-SNARE complex is highly stable, resistant even to a membrane solubilizing anionic detergent, sodium dodecyl sulphate. Therefore, following membrane solubilization (Fig. 1B, D), the stable SNARE complexes [8] have enabled a detailed examination of its morphology at high resolution, using both AFM and electron microscopy (EM) in the current study.

Materials and methods

Protein purification

N-terminal 6 \times His-tag constructs for SNAP-25 and NSF, C-terminal 6 \times His-tag constructs for syntaxin 1A and VAMP2 were generated. All four proteins were expressed with 6xHis at full length in *Escherichia coli* (BL21DE3) and isolated by Ni-nickel-nitrilotriacetic acid affinity chromatography (Qiagen, Valencia, CA, USA). Protein concentration was determined by bicinchoninic acid (BCA) assay.

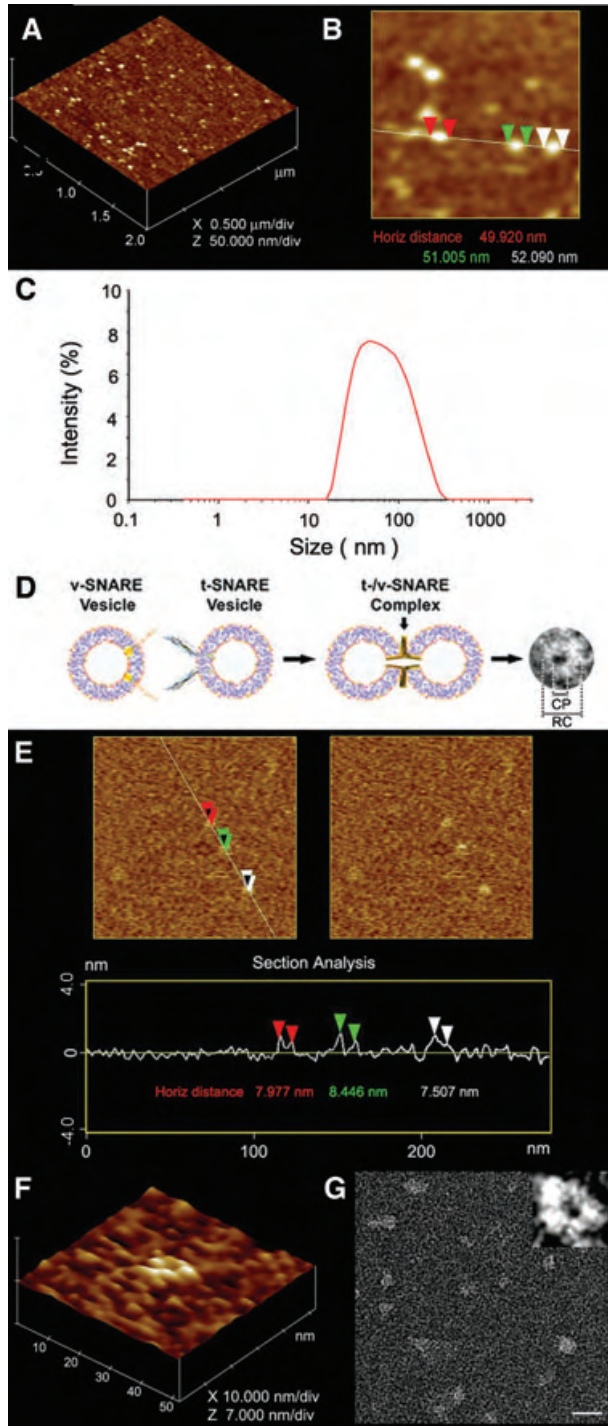


Fig. 2 Atomic force micrographs of PC:PS vesicles extruded through a membrane of 50 nm pore size. **(A)** Low-resolution image of PC:PS vesicles in buffer on mica surface. **(B)** High-resolution image of PC:PS vesicles in buffer on mica surface. Section analysis through three PC:PS vesicles demonstrating each of them to measure approximately 50 nm in diameter. **(C)** PCS demonstrating the average vesicle size to be approximately 50 nm. **(D)** Schematic drawing of a v-SNARE proteoliposome, shown interacting with a t-SNARE proteoliposome, to form a t-v-SNARE ring complex (RC) having a central pore (CP) or channel. **(E)** Low-resolution atomic force micrographs of the SNARE ring complex on mica surface in buffer. Note in the AFM section analysis of the 7.5–8.466 nm diameter t-v-SNARE ring complexes formed when approximately 50 nm diameter t-SNARE-reconstituted vesicles and 50 nm diameter v-SNARE-reconstituted vesicles meet. **(F)** A high-resolution AFM image of the t-v-SNARE ring complex. **(G)** Low-resolution electron micrograph of the t-v-SNARE ring complexes (Bar = 20 nm). The inset is an EM micrograph of a 7.5 nm diameter t-v-SNARE ring complex within a 10 nm box.

phatidylcholine: 1,2-dioleoyl phosphatidylserine in 70:30 mol/mol ratios in glass test tubes. The lipid mixture was dried under gentle stream of nitrogen and resuspended in decane. Lipids were suspended in 5 mM sodium phosphate buffer, pH 7.5, by vortexing for 5 min. at room temperature. Unilamellar vesicles were formed following five times sonications for 2 min./sonication, followed by passing the resultant liposomes through a 50 nm pore size membrane using an extruder. Typically, vesicles ranging in sizes from 48 to 52 nm diameter were obtained as assessed by AFM and photon correlation spectroscopy (PCS) (Fig. 2A–C). Proteoliposomes were prepared by gently mixing either t-SNARE complex (equal amounts of syntaxin 1-His₆ and His₆-SNAP-25, final concentration 25 μM) or VAMP2-His₆ (final concentration 25 μM) with liposomes [4–7], followed by three freeze/thaw cycles to enhance protein reconstitution at the vesicles membrane. PCS was performed for the measurement of proteoliposome size [6], using a Zetasizer Nano ZS, (Malvern Instruments, Worcestershire, UK).

Atomic force microscopy of the t-v-SNARE complex

AFM was performed on phosphatidylcholine:phosphatidylserine (PC:PS) vesicles and on the membrane-directed t-v-SNARE complexes obtained following vesicle solubilization (Figs 1 and 2). Samples were placed on mica surface in buffer for AFM imaging. The complexes were imaged using the Nanoscope IIIa AFM from Veeco Instruments Inc. (Plainview, NY, USA). Images were obtained in the ‘tapping’ mode in fluid, using silicon nitride tips with a spring constant of 0.38 N/m, and an imaging force of <200 pN. Images were obtained at line frequencies of 2 Hz, with 512 lines per image, and constant image gains. Topographical dimensions of the lipid vesicles and the resultant t-v-SNARE ring complexes were analysed using the software nanoscope IIIa4.43r8, supplied by Digital Instruments.

Vesicle size measurements using photon correlation spectroscopy

Changes in SV size were determined using PCS. PCS is a well-known technique for the measurement of size of micrometre to nanometre size particles and macromolecules. PCS measurements (Fig. 2C) were performed in a Zetasizer Nano ZS, (Malvern Instruments). In a typical experiment, the

Preparation of proteoliposomes

All lipids were obtained from Avanti Polar Lipids (Alabaster, AL, USA). A 5 mM lipid stock solution was prepared by mixing 1,2-dioleoyl phos-

size distribution of isolated SVs was determined using built-in software provided by Malvern Instruments. Prior to determination of the vesicle hydrodynamic radius, calibration of the instrument was performed with latex spheres of known size. In PCS, subtle fluctuations in the sample scattering intensity are correlated across microsecond time scales. The correlation function was calculated, from which the diffusion coefficient was determined. Using Stokes–Einstein equation, hydrodynamics radius can be acquired from the diffusion coefficient [9]. The intensity size distribution, which is obtained as a plot of the relative intensity of light scattered by particles in various size classes, is then calculated from a correlation function using built-in software. The particle scattering intensity is proportional to the molecular weight squared. Volume distribution can be derived from the intensity distribution using Mie theory [10, 11]. The transforms of the PCS intensity distribution to volume distributions can be obtained using the provided software by Malvern Instruments.

Electron microscopy of the t-/v-SNARE complex

EM was performed with a Tacnai 20 electron microscope (Philips Electron Optics/FEI, Eindhoven, The Netherlands) operating at 200 kV. Aliquots (~2.5 μ l) were adhered to thin pure carbon-coated 300-mesh copper grids, which had been rendered hydrophilic by glow discharge for 20 sec. The grids were washed with drops of deionized water and then exposed to drops of 2% (w/v) uranyl formate as previously reported [12]. Images at 80,000 \times magnification were recorded at low defocus on 4 K \times 4 K Gatan UltraScan charge-coupled device (Gatan Inc., Pleasanton, CA, USA) under low electron dose conditions (Figs 2–4). Each pixel of the micrographs corresponds to 1.4 Å at the level of the specimen. Particles in micrographs were selected and windowed using EMAN software [13].

Contour mapping of the t-/v-SNARE ring complex: To display the protein structure at greater detail, contour maps of the t-/v-SNARE protein ring complex was obtained using SPIDER software [14]. All particles were first normalized using a mean density of 0 and standard deviation of 10, then, contoured by the lowest ring at 1.0. Outside the protein complex, the background is flattened and smoothed. The protein boundary is defined by the darkest shadow around the particles, which results from the contrast transfer function of electrons.

Topography of the t-/v-SNARE ring complex from electron density maps: Heavy metal staining of the t-/v-SNARE complex enables an estimation of the relative size and arrangement of proteins in electron micrographs of the complex. Thus, intensity of negative stained proteins in electron micrographs, reflect the dimension, concentration and arrangement of protein at the various locations. Higher intensity in the micrographs corresponds to greater amount of protein at that location. Using CHIMERA software developed at the University of California, San Francisco [15, 16], protein density distributions were determined and revealed in three dimensions. Here, the colours from blue, green, yellow to red, (or from dark, grey to white) correspond to the protein image intensity from lowest to the highest (Figs 3 and 4). The highest peak in each image is presented at 30 pixels. Stereo views of the t-/v-SNARE ring complex topographies were obtained by utilizing the wall-eye stereo view created by UCSF Chimera [15, 16].

Histograms of the intensity distribution of electron density maps of t-/v-SNARE ring complex: The intensity of the density map was linearly normalized from 0 to 1. The histograms of the normalized intensity were generated and displayed based on a sampling step of 0.05. The similarity of the histogram may correspond to the similarity of the topological structure of the t-/v-SNARE ring complex.

Intensity distribution along the centre horizontal line of the t-/v-SNARE ring complex: Analogous to section analysis by the AFM, 1D intensity dis-

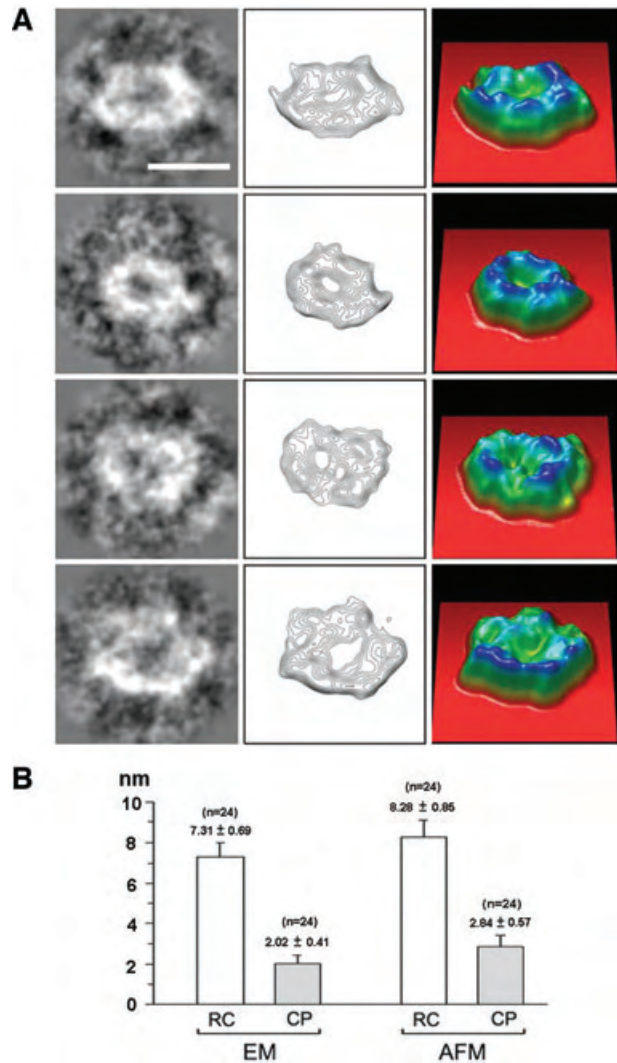


Fig. 3 Electron micrograph (A, left column), electron density map (A, centre column), and 3D contour map (A, right column) of isolated t-/v-SNARE ring complex formed when 50 nm diameter t-SNARE-reconstituted vesicles and 50 nm diameter v-SNARE-reconstituted vesicles meet (Bar = 7 nm). (B) Vertical bars indicate SEM. Note the 8.28 \pm 0.85 nm diameter hydrated SNARE ring complex (RC) having a 2.84 \pm 0.57 nm diameter central pore (CP) within. In contrast, dehydrated SNARE ring complex from the same preparation, examined using EM, measure 7.31 \pm 0.69 nm, and its central pore 2.02 \pm 0.41 nm diameter.

tribution across the centre of the t-/v-SNARE ring complex provides pixel intensities at various positions of the structure. The intensity presented is the average of 9 pixels wide stripe across the centre of the particle.

Mathematical prediction of SNARE ring complex size

Employing standard mathematical formula for the volume and surface areas of spheres one could estimate and predict the contact surface and the resultant size of t-/v-SNARE complexes formed.

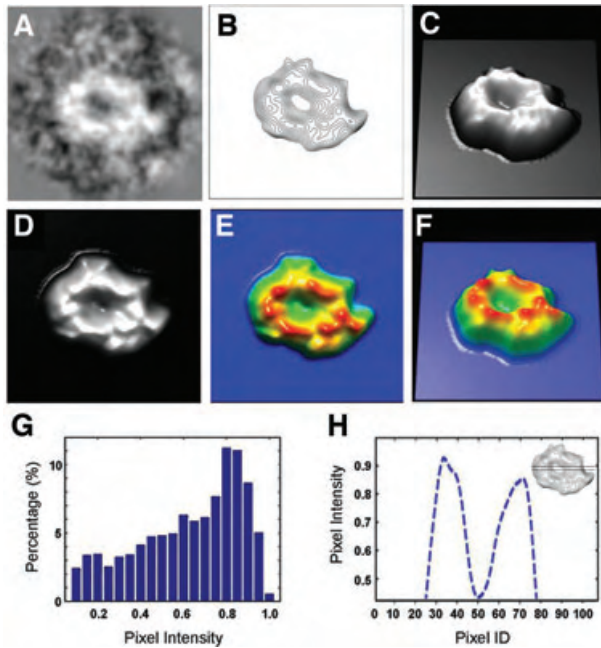


Fig. 4 Electron micrographs (A), electron density maps (B), and 3D contour maps (C) of isolated t-v-SNARE ring complexes formed when approximately 50 nm diameter t-SNARE-reconstituted vesicles and 50 nm diameter v-SNARE-reconstituted vesicles interact. 3D topography of t-v-SNARE obtained from their corresponding electron maps. The colours from blue, through green to red; and from black, through grey to white, correspond to the protein image density from lowest to the highest. The highest peak in each image represents 30 pixels (1.4 Å/pixel). Box size = 15 nm. (D–F) Wall-eye stereo view of the 3D topographies of SNARE ring complexes is presented. (G) Histogram of the intensity of a t-v-SNARE ring complex is shown. The similarity between the histograms may correspond to the similarity between the topological structures of the complex. (H) One-dimensional intensity distribution along the horizontal direction of a SNARE ring complex, similar to an AFM section analysis. The intensity distribution represents an average of 9 pixels wide stripe taken across the centre of a SNARE ring complex. Note the central channel in the intensity distribution map.

Synaptic vesicle isolation

SVs were prepared from rat brains using published procedures [17, 18]. Whole brain from Sprague-Dawley rats, weighing 100–150 g, was isolated and placed in ice-cold buffered sucrose solution (5 mM HEPES [4-(2-hydroxyethyl)-1-piperazineethanesulfonic acid], pH 7.4, 0.32 M sucrose), supplemented with protease inhibitor cocktail (Sigma, St. Louis, MO, USA). The brain tissue was homogenized using 8–10 strokes in a Teflon-glass homogenizer. The total homogenate was centrifuged for 3 min. at $2500 \times g$, and the supernatant fraction was further centrifuged for 15 min. at $14,500 \times g$, to obtain a pellet. The resultant pellet was resuspended in buffered sucrose solution, and loaded onto a 3–10–23% Percoll gradient. After centrifugation at $28,000 \times g$ for 6 min., the enriched synaptosome fraction was collected at the 10–23% Percoll gradient interface. To isolate SVs, the synaptosome preparation was diluted using 9 vol of ice-cold water, resulting in the lysis of synaptosomes to release SVs,

followed by 30 min. incubation on ice. The homogenate was then centrifuged for 20 min. at $25,500 \times g$, and the resultant supernatant enriched in SVs was obtained.

Imaging synaptic vesicles and corresponding SNARE complexes

To observe physiological SNARE complexes on mica for AFM studies, freshly cleaved mica disks were placed in a fluid chamber. Two hundred microlitres of imaging buffer solution containing 140 mM NaCl, 10 mM HEPES and 1 mM CaCl_2 , was placed at the centre of the cleaved mica disk. Prior to deposition on mica, t-SNARE reconstituted vesicles were gently layered on the mica surface, and incubated at room temperature for 60 min. prior to washing. Isolated SVs were added, incubated for 20 min., prior to three washes using the imaging buffer. During repeated imaging of the SVs attached to the t-SNARE-membrane supported by mica, some SVs are dislodged by the AFM cantilever tip, exposing the t-v-SNARE ring complex (Fig. 5D).

Results and discussion

In the present study, recombinant full-length t-SNARE and v-SNARE proteins were expressed and purified for use according to published procedures [4–7, 19, 20]. As indicated earlier in the manuscript, because majority of intracellular fusion events occur between vesicular compartments, we set out to determine the structure and arrangement of the t-v-SNARE complex when t-SNARE-vesicles and v-SNARE-vesicles meet. Because both opposing membrane exhibit curvature, we expected the v- and t-SNAREs to interact at a point, attracting additional SNARE pairs to form a t-v-SNARE bundle. To our surprise, exposure of 50 nm v-SNARE-liposome to 50 nm t-SNARE-liposome resulted in the establishment of a highly stable approximately 8 nm diameter t-v-SNARE ring complex. Because t-v-SNARE complex is highly stable, resistant even to the membrane solubilizing anionic detergent, sodium dodecyl sulphate, allowed its examination at ultra high resolution, using both AFM and EM in the current study. AFM micrographs demonstrate the central pore within an 8.28 nm SNARE ring complex to measure 2.84 nm in diameter. Dehydrated SNARE ring complex from the same preparation examined using EM, measure 7.31 nm, and its central pore is 2.02 nm in diameter, suggesting a hydrated channel (Fig. 3). These measurements further demonstrate the thickness of the ring to be ~2.5 nm, and assuming the ring thickness to reflect the diameter of a unit t-v-SNARE pair, it would take approximately six SNARE pairs to form such a ring. Indeed, on close examination of the 3D contour maps obtained from EM micrographs, six such densities are identifiable (Figs 3 and 4). Because the highest peak in each 3D contour map was determined to represent 42 Å, each SNARE pair in the complex represents a rod measuring 4.2 nm in height and 2.5 nm in diameter (Fig. 5). On close examination, the ring complex leaves little room for additional SNARE pairs, imparting the ring a leak-proof contour. A possible mechanism in forming such tight

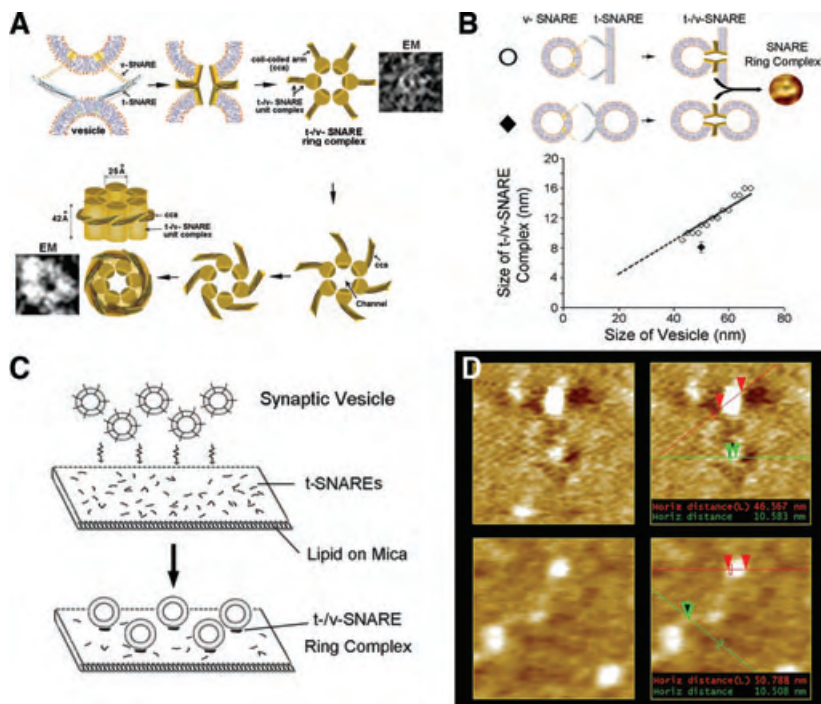


Fig. 5 The possible establishment of a leak-proof SNARE ring complex channel is demonstrated (A). Size of the t-/v-SNARE ring complex is directly proportional to the size of the SNARE-associated vesicle (B). Different sizes of v-SNARE-associated vesicles, when interacting with t-SNARE-associated membrane (○), demonstrate the SNARE ring size to be directly proportional to the vesicle size. When a 50 nm diameter v-SNARE-reconstituted vesicle interacts with a t-SNARE-reconstituted membrane, a 11 nm diameter t-/v-SNARE ring complex is formed. Similarly, the present study demonstrates that when a 50 nm diameter v-SNARE-reconstituted vesicle, interacts with a 50 nm diameter t-SNARE-reconstituted vesicle, an 8 nm diameter t-/v-SNARE ring complex is established (◆). Analogous to the 11 nm diameter t-/v-SNARE ring complexes formed when 50 nm v-SNARE vesicles meet a t-SNARE-reconstituted planer membrane (B), approximately 11 nm diameter t-/v-SNARE ring complexes are formed when 50 nm diameter SVs meet a t-SNARE-reconstituted planer membrane (C, D).

interactions between the SNARE pairs may involve a wrap-around of the hydrophilic coiled-coil t-/v-SNARE arm in each SNARE pair with its neighbour. This is suggested from EM images, where a section of each SNARE pair exhibits a splayed out and curved profile (Fig. 5).

Interestingly, the SNARE ring size can be predicted with reasonable accuracy. The formation of a t-/v-SNARE ring between interacting vesicles creates a flat circular zone of continuity within the ring, deforming the vesicles from their original spherical shapes into truncated spheres. If the volume of each vesicle remains constant, as we assume here, the deformation of the vesicles into truncated spheres will result in an increase in the surface area of each vesicle, which in turn produces a proportional increase in surface free energy. Employing standard mathematical formulae for the volume and surface areas of spheres and spherical caps, we find that the increase in surface area, ΔS , can be accurately approximated by the following equation for $a/R < 0.5$: $\Delta S = 0.254 (1/R_1^2 + 1/R_2^2) \pi a^4$, where R_1 and R_2 are the radii of the interacting vesicles, and a is the radius of the flat circular region of continuity, *i.e.* the t-/v-SNARE ring radius. Employing this formula for two vesicles of equal radius R_1 , we obtain $\Delta S = 0.508 \pi a^4 / R_1^2$. It could be assumed that the v- and t-SNAREs participating in the t-/v-SNARE ring were originally present within the membrane encompassed by the SNARE ring, and that these SNARE pairs are swept out to the circumference of the ring during the ring formation process (Fig. 1C). Binding energy is stored when a t-SNARE forms a complex with a v-SNARE to form a t-/v-SNARE pair. The total energy stored by the formation of a t-/v-SNARE ring is proportional to the number of t-/v-SNARE pairs in the ring, which in turn is proportional to the ring area πa^2 . In case

of SNARE ring formation to proceed as a spontaneous process, the energy stored by formation of t-/v-SNARE pairs must be greater than or equal to the increase in surface free energy, leading to a direct proportionality between ring area πa^2 and increase in surface area ΔS , as given by the formulas presented earlier. This proportionality can be exploited to develop the following equation relating the ring radius a_{12} , for fusion of vesicles of radii R_1 and R_2 , to the ring radius a_{11} produced by fusion of two equal-size vesicles of radius R_1 : $a_{12}/a_{11} = [2/(1 + R_1^2/R_2^2)]^{1/2}$. In case of fusion of a vesicle of radius R_1 with a supported planar bilayer, where $R_2 \rightarrow \infty$, we obtain $a_{1\infty}/a_{11} = (2)^{1/2}$. Using the 8 nm t-/v-SNARE ring diameter established as a result of the interaction between 50 nm t-SNARE and v-SNARE vesicles, we are able to predict a 11.3 nm diameter t-/v-SNARE ring complex formed when 50 nm v-SNARE vesicles meet a t-SNARE-reconstituted planer membrane. This calculated diameter of 11.3 nm is in agreement with the 11 nm ring complex determined from experiments [5].

To further test if native SVs measuring approximately 50 nm in diameter (Fig. 5D), and containing v-SNARE at the membrane surface also form t-/v-SNARE ring complex, isolated SVs were exposed to a t-SNARE-reconstituted membrane supported by mica. Interestingly, similar to the 11 nm diameter t-/v-SNARE ring complex formed when 50 nm v-SNARE vesicles meet a t-SNARE-reconstituted planer membrane (Fig. 5B), approximately 11 nm diameter t-/v-SNARE ring complex is formed when 50 nm diameter SVs meet a t-SNARE-reconstituted planer membrane (Fig. 5D). This is the first demonstration of the formation of SNARE ring complex, when native secretory vesicles interact with t-SNAREs in a supported membrane, in further confirmation of the SNARE ring complex assembly.

It is also important to be aware that both membrane curvature and lipid composition, influence the size of the membrane-directed t-/v-SNARE assembly. In a recent study [21], we report for the first time that membrane-curvature-influencing lipids profoundly influence SNARE complex size and its disassembly. Approximately 11% smaller t-/v-SNARE ring complexes formed using 50 nm cholesterol-associated vesicles, as opposed to lysophosphatidylcholine (LPC)-associated vesicles. Modulating the concentration and distribution of such non-bilayer lipids at various membranes, could regulate the degree and rate of membrane fusion and membrane-directed SNARE complex assembly-disassembly. Cells with higher membrane-cholesterol levels, would promote membrane fusion whereas cells with increased membrane LPC content would facilitate secretory event longevity by inhibiting SNARE-complex disassembly. LPC is known to be elevated in cancer patients, and has been suggested for use as a

potential tumour marker. Therefore membrane fusion, a critical process in cells is likely to be impaired in cancers expressing elevated levels of LPC.

Acknowledgements

Financial support from NSF CBET-0730768 (J.J.P., C.W.M., B.P.J.), NIH NS-39918 (B.P.J.) and Wayne State Univ. Research Enhancement Program (B.P.J.), is gratefully acknowledged.

Conflict of interest

The authors confirm that there are no conflicts of interest.

References

1. Oylar GA, Higgins GA, Hart RA, *et al.* The identification of a novel synaptosomal-associated protein, SNAP-25, differentially expressed by neuronal subpopulations. *J Cell Biol.* 1989; 109: 3039–52.
2. Bennett MK, Calakos N, Scheller RH. Syntaxin: a synaptic protein implicated in docking of synaptic vesicles at presynaptic active zones. *Science.* 1992; 257: 255–9.
3. Trimble WS, Cowam DM, Scheller RH. VAMP-1: a synaptic vesicle-associated integral membrane protein. *Proc Natl Acad Sci USA.* 1988; 85: 4538–42.
4. Cho SJ, Kelly M, Rognien KT, *et al.* SNAREs in opposing bilayers interact in a circular array to form conducting pores. *Biophys J.* 2002; 83: 2522–7.
5. Cho WJ, Jeremic A, Jena BP. Size of supramolecular SNARE complex: membrane-directed self-assembly. *J Am Chem Soc.* 2005; 127: 10156–7.
6. Cook JD, Cho WJ, Stemmler TL, *et al.* Circular dichroism (CD) spectroscopy of the assembly and disassembly of SNAREs: the proteins involved in membrane fusion in cells. *Chem Phys Lett.* 2008; 462: 6–9.
7. Jeremic A, Quinn AS, Cho WJ, *et al.* Energy-dependent disassembly of self-assembled SNARE complex: observation at nanometer resolution using atomic force microscopy. *J Am Chem Soc.* 2006; 128: 26–2.
8. Yang B, Gonzalez Jr L, Prekeris R, *et al.* SNARE interactions are not selective. Implications for membrane fusion specificity. *J Biol Chem.* 1999; 274: 5649–53.
9. Pecora R. Dynamic light scattering: applications of photon correlation spectroscopy. New York; Plenum Press: 1985.
10. Mie G. Considerations on the optics of turbid media, especially colloidal metal sols. *Ann Physik.* 1908; 4: 377–442.
11. Matsuzaki K, Murase O, Sugishita K, *et al.* Optical characterization of liposomes by right angle light scattering and turbidity measurements. *Biochem Biophys Acta.* 2000; 1467: 219–26.
12. Ohi M, Li Y, Cheng Y, *et al.* Negative staining and image classification – powerful tools in modern electron microscopy. *Biol Proc.* 2004; Online 6: 23–34.
13. Ludtke SJ, Baldwin PR, Chiu WJ. EMAN: semiautomated software for high-resolution single-particle reconstructions. *Struct Biol.* 1999; 128: 82–97.
14. Frank J, Radermacher M, Penczek P, *et al.* SPIDER and WEB: processing and visualization of images in 3D electron microscopy and related fields. *Struct Biol.* 1996; 116: 190–9.
15. Pettersen EF, Goddard TD, Huang CC, *et al.* UCSF Chimera—a visualization system for exploratory research and analysis. *Comput Chem.* 2004; 25: 1605–12.
16. Goddard TD, Huang CC, Ferrin TE. Software extensions to UCSF chimera for interactive visualization of large molecular assemblies. *Structure.* 2005; 13: 473–82.
17. Kelly M, Cho WJ, Jeremic A, *et al.* Vesicle swelling regulates content expulsion during secretion. *Cell Biol Int.* 2004; 28: 709–16.
18. Jeremic A, Cho WJ, Jena BP. Involvement of water channels in synaptic vesicle swelling. *Exp Biol Med.* 2005; 230: 674–80.
19. Weber T, Zemelman BV, McNew JA, *et al.* SNAREpins: minimal machinery for membrane fusion. *Cell.* 1998; 92: 759–72.
20. Fasshaur D, Eliason WK, Brunger AT, *et al.* Identification of a minimal core of the synaptic SNARE complex sufficient for reversible assembly and disassembly. *Biochemistry.* 1998; 37: 10354–62.
21. Shin L, Cho WJ, Cook J, *et al.* Membrane lipids influence protein complex assembly-disassembly. *J Am Chem Soc.* 2010; 132: 5596–7.